Synthesis, Properties and Crystal Structures of $[Ru^{III}_2(tacn)_2(\mu\text{-}OH)_2(\mu\text{-}CO_3)]Br_2\cdot 3.75H_2O$ and $[Ru^{3.5}_2(dtne)(\mu\text{-}O)_2(\mu\text{-}CO_3)]PF_6\cdot 5H_2O$ [tacn = 1,4,7-triazacyclononane, dtne = 1,2-bis(1,4,7-triazacyclononan-1-yl)ethane] †

Arnd Geilenkirchen,[a] Peter Neubold,[a] Ralf Schneider,[a] Karl Wieghardt,*[,a] Ulrich Flörke,[b] Hans-Jürgen Haupt[b] and Bernhard Nuber[c]

[a] *Lehrstuhl für Anorganische Chemie I, Ruhr-Universität, D-44780 Bochum, Germany*

[b] *Anorganische und Analytische Chemie der Universität-Gesamthochschule, D-33098 Paderborn, Germany*

[c] *Anorganisch-Chemisches Institut der Universität, D-69120 Heidelberg, Germany*

The mono- and di-nuclear complexes $[Ru^{III}(tacn)Cl_3]$ **1**, $[Ru^{III}_2(dtne)Cl_6]$ **2**, and $[Ru^{III}_2(dtne)Br_6]$ **3** have been synthesised from $[Ru^{II}(dmso)_4Cl_2]$ (dmso = dimethyl sulfoxide), the respective amine and concentrated HCl or HBr in the presence of air where tacn and dtne represent 1,4,7-triazacyclononane and 1,2-bis(1,4,7-triazacyclononan-1-yl)ethane. The compounds proved to be useful starting materials for the hydrolytic generation of hydroxo/oxo-bridged dinuclear Ru^{III}_2 and $Ru^{III}Ru^{IV}$ species in aqueous solution containing sodium carboxylates or sodium carbonate. The diamagnetic red-purple species $[Ru^{III}_2(dtne)(\mu\text{-}OH)_2(\mu\text{-}PhCO_2)][PF_6]_3$ **4** and its green μ-carbonato analogue $[Ru^{III}_2(tacn)_2(\mu\text{-}OH)_2(\mu\text{-}CO_3)]Br_2\cdot 3.75H_2O$ **5** were prepared. Replacement of the μ-carboxylato bridge in **4** by a $\mu\text{-}CO_3^{2-}$ bridge in the presence of air gave green crystals of the mixed-valent species $[Ru^{3.5}_2(dtne)(\mu\text{-}O)_2(\mu\text{-}CO_3)]PF_6\cdot 5H_2O$ **6**. Complexes **5** and **6** have been structurally characterized by X-ray crystallography; both contain a bioctahedral edge-sharing unit of $Ru^{III}_2(\mu\text{-}OH)_2(\mu\text{-}CO_3)^{2+}$ and $Ru^{3.5}(\mu\text{-}O)_2(\mu\text{-}CO_3)^{+}$, respectively, with Ru–Ru metal–metal bonds [2.560(1) in **5**, 2.469(1) in **6**]. The Ru^{IV}_2 analogues of **5** and **6** have been generated chemically and electrochemically in solution. The UV/VIS spectra, magnetic properties and the electrochemistry of **4**–**6** are reported.

In recent years the co-ordination chemistry of oxo/hydroxo-bridged dinuclear ruthenium complexes containing 'innocent' O,N-donor ligands has attracted much interest. One of the most fascinating aspects of this work has been the discovery that in edge- (**B**) and face-sharing (**C**) bioctahedral compounds the oxidation states can vary between **II** and **V** including of course a series of mixed-valent species.[1,2] In edge- and face-sharing compounds metal–metal bonding has been observed for ruthenium-(III), -(IV) and -(V), whereas one of the ruthenium(V) species reported by Bercaw and co-workers[3] appears to lack such interaction. Also of interest in this respect is a comparison of the structural and electronic features of types **D** and **E**[4] where **D** forms Ru–Ru bonds (≈2.55 Å) whereas in **E** the metal–metal interactions are very weak if present at all (Ru···Ru > 3.1 Å).

In previous work[1,2a,b,4a] we have shown that many complexes containing mainly ruthenium(III) ions of types **B**, **D** and **E** are synthetically readily available *via* hydrolysis of mononuclear ruthenium(III) precursor complexes in aqueous solution which at times contained bridging carboxylates. The precursors contain co-ordinated tridentate cyclic amines as blocking groups for three facial sites of a regular octahedron. 1,4,7-Triazacyclononane (tacn) and its *N*-methylated derivative 1,4,7-trimethyl-1,4,7-triazacyclononane (tmtacn) proved to be ideally suited for this purpose due to their enormous kinetic and thermodynamic stability once bound to a metal. This stability may be still further enhanced by using the potentially binucleating, strapped derivative 1,2-bis(1,4,7-triazacyclononan-1-yl)ethane[5] (dtne) the co-ordination chemistry of which has not been fully exploited to date. The goal of the present work was to develop synthetic routes to ruthenium complexes of type **D** with metal oxidation states > III. Meyer and co-workers[4e] had shown that replacement of two carboxylato bridges in complexes of type **E** by two more negatively charged carbonato bridges makes the +**IV** oxidation state of ruthenium more accessible by 300–400 mV. It appeared interesting to us to test this for complexes of type **D**. The synthesis of $[Ru^{III}_2(tacn)_2(\mu\text{-}OH)_2(\mu\text{-}MeCO_2)]^{3+}$ has been reported by our laboratory previously.[1] Here we replace two tacn ligands by dtne and the acetate by a μ-carbonato bridge.

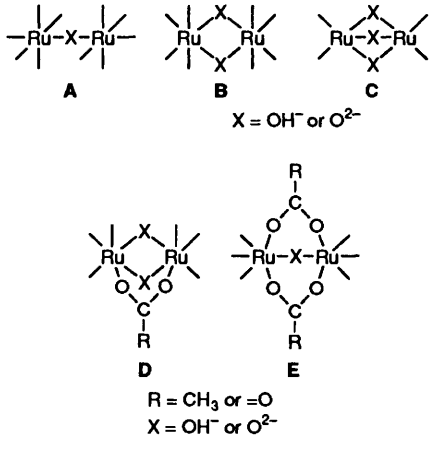

† *Supplementary data available:* see Instructions for Authors, *J. Chem. Soc., Dalton Trans.*, 1994, Issue 1, pp. xxiii–xxviii.

Non-Si unit employed: $\mu_B \approx 1.927 \times 10^{-24}$ J T^{-1}.

Experimental

Materials and Methods.—The preparations of the ligands 1,4,7-triazacyclononane[6] and 1,2-bis(1,4,7-triazacyclononan-1-yl)ethane[5] and of the complex $[Ru^{II}(dmso)_4Cl_2]$[7] (dmso = dimethyl sulfoxide) have been described in the literature. All other chemicals were obtained from commercial sources and used as supplied. Infrared spectra were recorded on a Perkin Elmer FT IR 1720X spectrometer as KBr discs, electronic spectra on a Perkin Elmer Lambda 9 UV/VIS/NIR spectrophotometer in the range 200–1500 nm. Cyclic voltammograms were recorded on PAR equipment consisting of a model 173/179 potentiostat/galvanostat with a model 175 universal programmer. The ESR spectrum was recorded on a Bruker ER 200 ESR spectrometer.

Preparation of Complexes.—$[Ru^{III}(tacn)Cl_3]$ **1**. The preparation of this complex has been described previously.[1] An improved synthesis is given here. To $[Ru(dmso)_4Cl_2]$ (1.45 g, 3.0 mmol) in dry toluene (60 cm^3) was added tacn (0.39 g, 3.02 mmol). The mixture was heated to reflux for 1 h. After cooling to 0 °C, the grey residue of $[Ru(dmso)_2(tacn)Cl]Cl$ was filtered off and dissolved in concentrated HCl (20 cm^3). Heating to reflux in the presence of air for 10 min initiated the precipitation of orange-red microcrystals of **1** which were filtered off, washed with ethanol and diethyl ether and air-dried (yield: 0.95 g, 94%).

$[Ru^{III}_2(dtne)Cl_6]$ **2**. A suspension of $[Ru(dmso)_4Cl_2]$ (0.97 g, 2.0 mmol) and dtne (0.285 g, 1.0 mmol) in water-free ethanol (50 cm^3) was heated to reflux for 24 h. The cooled solution was filtered. The yellow residue was immediately suspended in concentrated HCl (20 cm^3). The mixture was heated to reflux for 15 min in the presence of air. Orange-red microcrystals formed and filtered off, washed with ethanol and air-dried (yield: 0.20 g, ≈30%) (Found: C, 23.7; H, 4.4; Cl, 29.7; N, 12.0. Calc. for $C_{14}H_{32}Cl_6N_6Ru_2$: C, 24.05; H, 4.55; Cl, 30.4; N, 12.05%).

$[Ru^{III}_2(dtne)Br_6]$ **3**. This complex was prepared as described above for **2** with the following modifications. The yellow intermediate was suspended in concentrated HBr (48%, 25 cm^3) and heated to reflux for 45 min in the presence of air. Upon cooling to 0 °C, brown-red microcrystals of **2** were obtained in ≈30% yield (Found: C, 17.6; H, 3.6; N, 8.7. Calc. for $C_{14}H_{32}Br_6N_6Ru_2$: C, 17.4; H, 3.3; N, 8.7%).

$[Ru^{III}_2(dtne)(\mu\text{-}OH)_2(\mu\text{-}PhCO_2)][PF_6]_3$ **4**. A suspension of complex **2** (0.10 g, 0.14 mmol) and sodium benzoate (1.0 g) in water (40 cm^3) was heated to 60 °C for 1 h after which time a deep red-purple, clear solution was obtained. Addition of $NaPF_6$ (1.0 g) and cooling to 0 °C initiated the precipitation of red-purple microcrystals which were filtered off. Recrystallization from hot water produced **4** in 30% yield (Found: C, 24.0; H, 3.8; N, 7.6; P, 8.9. Calc. for $C_{21}H_{39}F_{18}N_6O_4P_3Ru_2$: C, 23.5; H, 3.6; N, 7.8; P, 8.9%).

$[Ru^{III}_2(tacn)_2(\mu\text{-}OH)_2(\mu\text{-}CO_3)]Br_2\cdot 3.75H_2O$ **5**. A suspension of complex **1** (0.50 g, 1.5 mmol) and $NaHCO_3$ (1.0 g) in water (50 cm^3) was heated to 80 °C for 30 min after which time a clear green solution was obtained. Addition of NaBr (1.0 g) and cooling initiated the precipitation of green crystals which were recrystallized from hot water (yield: 60%). The corresponding iodide, tetrafluoroborate, tetraphenylborate, or hexafluorophosphate salts may be isolated by addition of the respective sodium salt to the above green solution (Found: C, 20.0; H, 5.1; Br, 20.1; N, 10.7. Calc. for $C_{13}H_{39.5}Br_2N_6O_{8.75}Ru_2$: C, 20.0; H, 4.6; Br, 20.4; N, 10.5%).

$[Ru^{3.5}_2(dtne)(\mu\text{-}O)_2(\mu\text{-}CO_3)]PF_6\cdot 5H_2O$ **6**. A solution of sodium acetate (2.0 g) and complex **2** (0.35 g, 0.50 mmol) in water (20 cm^3) was heated to 60 °C for 1 h. To the now deep red solution was added an alkaline (pH ≈10) aqueous solution (5 cm^3) of $NaPF_6$ (1.0 g). The combined solutions were added dropwise to a solution of Na_2CO_3 (1.5 g) and NaOH (0.5 g) in water (20 cm^3). A colour change from red to brown-green was observed. Air was bubbled through this solution for 2 h. Upon standing of the solution in an open vessel for 2–3 d greenish crystals precipitated which were recrystallized from alkaline aqueous, carbonate and $NaPF_6$ containing solutions. The green needles loose water of crystallization upon storage *in vacuo* over P_4O_{10} and become turbid. The yields were quite low (≈10% based on **2**) (Found: C, 22.0; H, 4.9; N, 10.1. Calc. for $C_{15}H_{42}F_6N_6O_{10}PRu_2$: C, 22.1; H, 5.2; N, 10.3%).

Crystal Structure Analyses.—Table 1 summarizes the relevant data for the crystal structure determinations. Final atom coordinates are given in Tables 2 and 3 for complexes **5** and **6**, respectively. Intensity data were corrected for Lorentz, polarization and absorption effects in the usual manner. The structures were solved by conventional Patterson and Fourier difference methods by using the SHELXTL-PLUS program package.[8] The function minimized during full-matrix least-squares refinement was $\Sigma w(|F_o| - |F_c|)^2$. Neutral atom scattering factors and anomalous dispersion corrections for non-hydrogen atoms were taken from ref. 9. The positions of the hydrogen atoms of the methylene groups were calculated and included with fixed isotropic thermal parameters. All other atoms with the exception of the carbon atoms in **6** were refined with anisotropic thermal parameters. The PF_6^- anions in **6** were found to be slightly disordered. This disorder could not be modelled satisfactorily by a split-atom model.

Additional material available from the Cambridge Crystallographic Data Centre comprises H-atom coordinates, thermal parameters and remaining bond lengths and angles.

Results and Discussion

Syntheses and Characterization of Complexes.—The reaction of $[Ru(dmso)_4Cl_2]$ and the cyclic amine 1,4,7-triazacyclononane or its strapped analogue 1,2-bis(1,4,7-triazacyclononan-1-yl)ethane in toluene or ethanol affords yellow precipitates of presumably $[Ru(tacn)(dmso)_2Cl]Cl$ and $[Ru_2(dtne)(dmso)_4Cl_2]Cl_2$ in nearly quantitative yields. These precursor materials react with concentrated hydrochloric or hydrobromic acid under reflux in the presence of air with formation of brown-red microcrystalline products of $[Ru(tacn)Cl_3]$ **1**, $[Ru_2(dtne)$-

Table 1 Crystal data and data collection parameters for the structures of complexes **5** and **6**

	5	**6**
Molecular formula	$C_{13}H_{32}Br_2N_6O_5Ru_2\cdot 3.75H_2O$	$C_{15}H_{32}F_6N_6O_5PRu_2\cdot 5H_2O$
M	781.9	813.6
Crystal size/mm	0.09 × 0.34 × 0.09	0.055 × 0.06 × 0.38
a/Å	8.042(5)	7.645(1)
b/Å	11.656(7)	11.402(3)
c/Å	15.433(9)	16.763(6)
α/°	111.62(4)	79.27(1)
β/°	89.78(5)	82.47(1)
γ/°	105.47(5)	85.42(1)
U/Å^3	1288.9	1421
D_c/g cm^{-3}	2.01	1.902
$F(000)$	775	822
μ(Mo-Kα)/cm^{-1}	4.27	11.92
Diffractometer	AED II (Siemens)	Nicolet R3m/V
2θ range/°	3–60	3–55
Reflections measured	7566	6591
Observed reflections (criterion)	4412 [$I \geqslant 2.5\sigma(I)$]	3959 [$I \geqslant 2.0\sigma(I)$]
Least-squares parameters	289	296
R	0.070	0.066
R'	0.059 [$w = 1/\sigma^2(F)$]	0.054 [$w = 1/\sigma^2(F) + 0.0001F^2$]

Details in common: T = 298 K; Mo-Kα radiation (λ = 0.710 73 Å); absorption correction, empirical ψ scans for complex **5**, numerical for **6**; ω–2θ scan; green needles; triclinic; space group $P\bar{1}$; Z = 2; $R = \Sigma(|F_o| - |F_c|)/\Sigma|F_o|$; $R' = [\Sigma(|F_o| - |F_c|)^2/\Sigma|F_o|^2]^{\frac{1}{2}}$.

Cl_6] **2**, and [Ru_2(dtne)Br_6] **3** (Scheme 1). Complexes **1**–**3** are paramagnetic with effective magnetic moments at room temperature which are indicative of an uncoupled low-spin d^5 electronic configuration of each ruthenium(III) ion (Table 4). They are nearly insoluble in all common organic solvents and water but proved to be excellent starting materials for the formation of dinuclear complexes *via* hydrolysis reactions.

In a previous study[1] we had shown that hydrolysis of complex **1** in aqueous solution containing the sodium salt of a carboxylic acid produces dinuclear, diamagnetic complexes of the type [Ru_2(tacn)$_2$(μ-OH)$_2$(μ-carboxylate)]$^{3+}$ of which the μ-acetato-bridged species has been structurally characterized by X-ray crystallography. In analogy to this work hydrolysis of **2** or **3** in water containing sodium benzoate at elevated temperatures yields a clear, red-purple solution from which upon addition of $NaPF_6$ red-purple, diamagnetic crystals of [Ru_2(dtne)(μ-OH)$_2$(μ-$PhCO_2$)][PF_6]$_3$ **4** are obtained. In the infrared spectrum ν_{asym}(CO) and ν_{sym}(CO) stretching frequencies are observed at 1541 and 1418 cm^{-1}, respectively. The difference of 123 cm^{-1} is taken as clear evidence for a symmetrical carboxylato bridge. The μ-acetato-bridged analogue [Ru_2(dtne)(μ-OH)$_2$(μ-$MeCO_2$)]$^{3+}$ may be prepared similarly by using sodium acetate.

When complex **1** is hydrolysed in an aqueous solution containing $NaHCO_3$ a clear green solution is obtained. Addition of NaBr initiates the precipitation of diamagnetic green crystals of [Ru_2(tacn)$_2$(μ-OH)$_2$(μ-CO_3)]Br_2·3.75H_2O **5** which is the μ-carbonato-bridged analogue of **4**. In the infrared spectrum ν(C–O) stretching frequencies of the bridging carbonate are observed at 1560 and 1423 cm^{-1}. The iodide, PF_6^-, BF_4^- or BPh_4^- salts may be prepared from aqueous solutions of **5** to which the sodium salt of the respective anion is added.

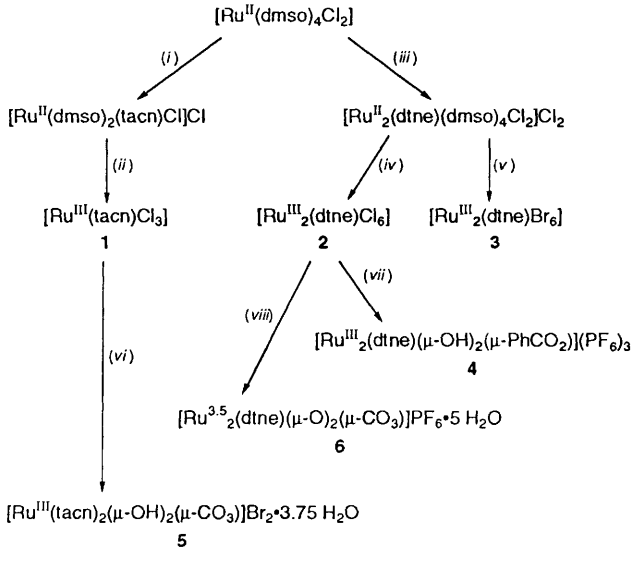

Scheme 1 (*i*) toluene, tacn; reflux 1 h; (*ii*) concentrated HCl, O_2; (*iii*) ethanol, dtne, reflux 24 h; (*iv*) concentrated HCl, O_2; (*v*) concentrated HBr, O_2; (*vi*) water–$NaHCO_3$, 80 °C, NaBr; (*vii*) water, sodium benzoate, 60 °C, $NaPF_6$; (*viii*) sodium acetate, water, 60 °C, $NaPF_6$, Na_2CO_3–NaOH

Table 2 Atom coordinates (× 10^4) for complex **5**

Atom	*x*	*y*	*z*
Ru(1)	3283(1)	6867(1)	1972(1)
Ru(2)	1028(1)	4855(1)	1986(1)
O(1)	3685(9)	5304(7)	2118(5)
O(2)	698(9)	6546(7)	2068(5)
C(0)	1965(14)	4779(11)	95(7)
O(3)	992(9)	4161(7)	526(5)
O(4)	2981(10)	5938(7)	520(5)
O(5)	1999(9)	4229(7)	−791(5)
N(1)	3397(12)	8593(8)	1890(6)
N(2)	5973(11)	7564(8)	1946(6)
N(3)	3936(11)	8033(8)	3387(6)
C(1)	4834(14)	8945(11)	1354(8)
C(2)	6453(15)	8759(11)	1736(8)
C(3)	6752(14)	7761(11)	2875(8)
C(4)	5855(14)	8531(11)	3657(7)
C(5)	3063(16)	9103(11)	3573(7)
C(6)	3445(16)	9669(11)	2814(8)
N(4)	853(12)	3032(9)	1984(7)
N(5)	761(12)	5274(9)	3402(6)
N(6)	−1629(12)	4112(8)	1864(6)
C(11)	1676(16)	3241(12)	2905(8)
C(12)	916(17)	4156(12)	3668(8)
C(13)	−976(14)	5535(12)	3552(7)
C(14)	−2332(15)	4439(12)	2785(8)
C(15)	−2110(15)	2969(11)	1337(8)
C(16)	−954(15)	2170(12)	1768(8)
Br(1)	2661(2)	878(2)	605(1)
Br(2)	2778(2)	7716(2)	5470(1)
O_w(1)	4720(12)	3691(8)	708(7)
O_w(2)	9820(11)	1617(8)	9076(7)
O_w(3)	452(18)	1084(15)	4617(9)
O_w(4)	3991(27)	3475(23)	4929(12)

Table 3 Atomic coordinates (× 10^4) for complex **6**

Atom	*x*	*y*	*z*
Ru(1)	1 700(1)	4 647(1)	6 841(1)
Ru(2)	468(1)	2 671(1)	7 343(1)
O(1)	2 898(8)	3 134(5)	7 295(4)
O(2)	−761(8)	4 222(5)	7 012(4)
N(1)	1 521(10)	5 378(6)	7 929(4)
N(2)	4 155(10)	5 436(6)	6 605(5)
N(3)	899(10)	6 402(6)	6 326(5)
N(4)	−1 954(11)	1 863(7)	7 469(5)
N(5)	1 294(11)	869(7)	7 751(5)
N(6)	−203(10)	2 655(7)	8 617(5)
C(14)	307(14)	4 844(9)	8 653(6)
C(15)	577(15)	3 566(9)	8 986(6)
C(1)	3 392(12)	5 324(9)	8 113(6)
C(2)	4 616(12)	5 819(8)	7 359(6)
C(3)	4 141(12)	6 411(8)	5 876(6)
C(4)	2 424(12)	7 168(9)	5 932(6)
C(5)	−164(12)	6 882(8)	7 002(6)
C(6)	848(13)	6 692(8)	7 722(6)
C(7)	−1 584(13)	642(9)	7 285(7)
C(8)	−129(15)	27(10)	7 749(7)
C(9)	1 811(15)	860(10)	8 590(7)
C(10)	385(14)	1 450(9)	9 076(7)
C(11)	−2 184(14)	2 820(9)	8 707(7)
C(12)	−2 994(14)	1 959(10)	8 286(7)
C(13)	1 472(11)	3 196(8)	5 555(5)
O(3)	1 988(8)	4 209(5)	5 691(4)
O(4)	897(8)	2 390(5)	6 163(4)
O(5)	1 560(8)	3 021(5)	4 833(4)
P	3 967(4)	2 291(3)	10 759(2)
F(1)	4 228(14)	958(8)	11 021(10)
F(2)	3 704(17)	3 609(9)	10 518(12)
F(3)	5 995(9)	2 415(8)	10 776(5)
F(4)	3 586(13)	2 431(15)	11 650(7)
F(5)	1 904(9)	2 137(8)	10 775(5)
F(6)	4 263(11)	2 230(13)	9 842(6)
O(6)	2 712(8)	5 687(5)	4 200(4)
O(7)	3 919(13)	−889(9)	7 159(7)
O(8)	5 536(14)	164(8)	5 699(7)
O(9)	8 864(16)	−760(8)	5 450(7)
O(10)	4 509(9)	7 726(6)	3 753(5)

Reaction of red $[Ru_2(dtne)(\mu\text{-}OH)_2(\mu\text{-}MeCO_2)]^{3+}$ which was prepared *in situ* from complex **2** and $Na(O_2CMe)$ in water with an alkaline aqueous solution of Na_2CO_3 and $NaPF_6$ in the presence of air at 60 °C affords a brown-greenish solution. From this solution green crystals of $[Ru_2(dtne)(\mu\text{-}O)_2(\mu\text{-}CO_3)]PF_6 \cdot 5H_2O$ **6** precipitate in low yields within 2–3 d at ambient temperature. In the infrared spectrum the ν(CO) stretching frequencies are observed at 1614 and 1500 cm^{-1}. Complex **6** is paramagnetic, and formally derived from the analogous species **5** by one-electron oxidation and concomitant deprotonation of the μ-hydroxo bridges. Fig. 1 shows the temperature dependence of the magnetic moment and molar susceptibility of **6** as determined by using a SQUID magnetometer. Corrections for underlying diamagnetism was applied with use of Pascal's constants. Magnetic moments between 1.91 μ_B at 295 K and 1.72 μ_B at 2.0 K per dinuclear unit clearly demonstrate the $S = \frac{1}{2}$ ground state of **6** which is in excellent agreement with the X-band ESR spectrum of a powdered sample of **6** recorded at 10 K (Fig. 2). A rhombic signal with g values at 2.33, 2.12 and 1.97 with no detectable hyperfine structure is observed.

Oxidation of complex **6** in aqueous solution by $[NH_4]_2[Ce(NO_3)_6]$, $Na_2S_2O_8$ or $KMnO_4$ generating the diruthenium(IV) species $[Ru_2(dtne)(\mu\text{-}O)_2(\mu\text{-}CO_3)]^{2+}$ is readily achieved. The resulting deep green solution shows an electronic absorption spectrum which is identical to that obtained electrochemically (Fig. 3) (see below). Attempts to isolate a crystalline material from such solutions failed. Complex **5** may be oxidized by a two-electron oxidation both chemically in aqueous solution by $[NH_4]_2[Ce(NO_3)_6]$ or electrochemically (see below). The electronic spectrum of the resulting deep green solution is very similar to that obtained for the oxidized species of **6**. Thus we propose that $[Ru_2(tacn)_2(\mu\text{-}O)_2(\mu\text{-}CO_3)]^{2+}$ is also a stable species in solution.

Crystal Structures.—Figs. 4 and 5 show the structures of the dication in crystals of complex **5** and of the monocation in **6**, respectively. Selected bond distances and angles are listed in Table 5. The structure of **5** consists of two distinct dinuclear

Table 4 Electronic spectral data and magnetic properties of the complexes

Complex	Solvent	λ_{max}/nm (ε/dm^3 mol^{-1} cm^{-1})	μ_{eff}(298 K)/μ_B
1		n.m.*	2.16
2		n.m.*	2.64
3		n.m.*	2.70
4	Acetone	258 (5500), 315 (sh), 516 (1200)	Diamagnetic
5	Water	263 (sh), 294 (14 000), 604 (14), 1085 (21)	Diamagnetic
6	Water	298 (2400), 1224 (406)	1.91

* n.m. = Not measured due to insolubility in all common solvents.

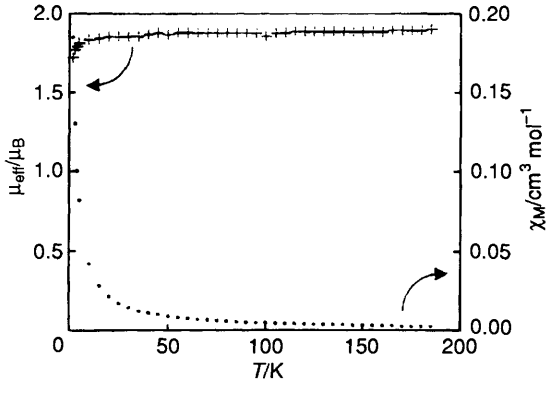

Fig. 1 Plot of the magnetic moment (+) and molar magnetic susceptibility (□) *vs.* temperature for a solid sample of complex **6**

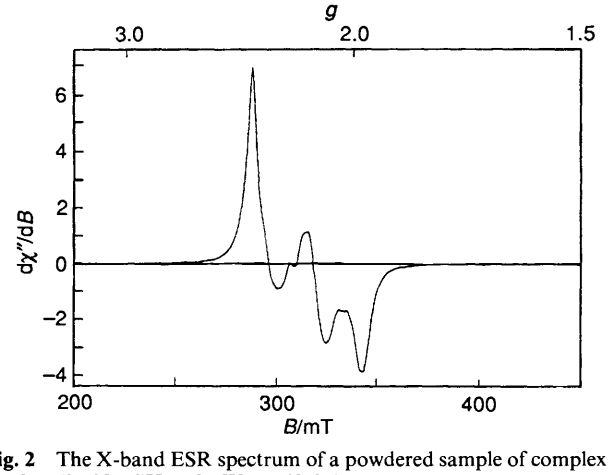

Fig. 2 The X-band ESR spectrum of a powdered sample of complex **6** at 10 K (9.4385 GHz, 20 μW per 40 dB)

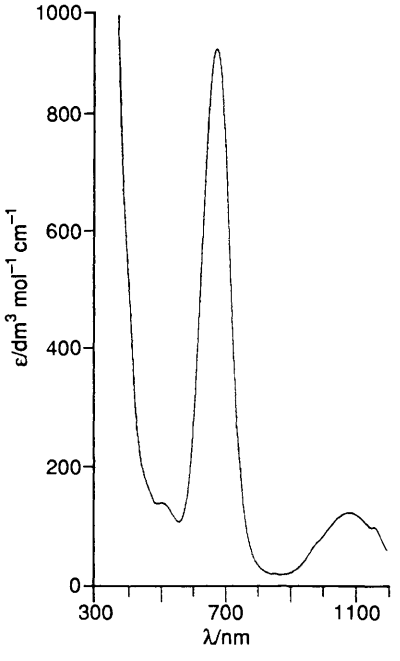

Fig. 3 The UV/VIS spectrum of an aqueous solution of complex **6** recorded after electrochemical one-electron oxidation at a potential of 0.07 V *vs.* NHE ([complex **6**] = 5.5 × 10^{-4} mol dm^{-3} in 0.10 mol dm^{-3} $LiClO_4$–water)

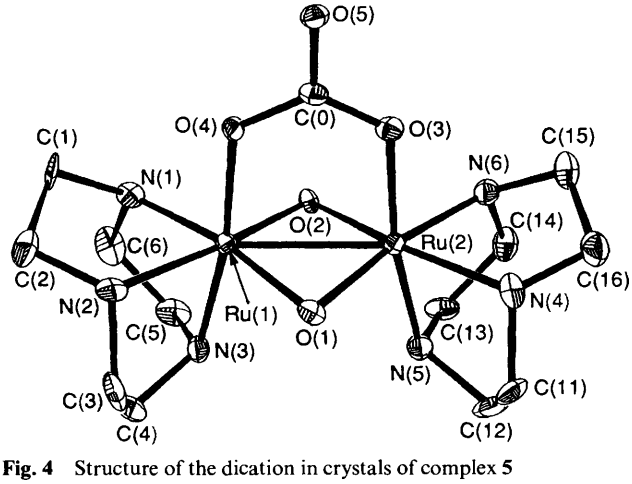

Fig. 4 Structure of the dication in crystals of complex **5**

Table 5 Selected bond distances (Å) and angles (°)

Complex **5**

Ru(1)–Ru(2)	2.560(1)	Ru(2)–O(2)	2.016(8)
Ru(1)–O(1)	2.022(9)	Ru(2)–O(3)	2.092(7)
Ru(1)–O(2)	2.026(7)	Ru(2)–N(4)	2.090(11)
Ru(1)–O(4)	2.081(6)	Ru(2)–N(5)	2.081(9)
Ru(1)–N(1)	2.041(11)	Ru(2)–N(6)	2.060(9)
Ru(1)–N(2)	2.104(9)	C(0)–O(3)	1.272(15)
Ru(1)–N(3)	2.081(7)	C(0)–O(4)	1.298(11)
Ru(2)–O(1)	2.052(7)	C(0)–O(5)	1.283(12)
O(1)–Ru(2)–O(2)	100.7(3)	O(2)–Ru(2)–O(3)	93.2(3)
O(2)–Ru(2)–O(3)	90.1(3)	O(2)–Ru(2)–N(4)	168.2(3)
O(1)–Ru(2)–N(4)	90.3(4)	O(2)–Ru(2)–N(5)	92.3(4)
O(1)–Ru(2)–N(5)	96.0(3)	O(2)–Ru(2)–N(6)	89.0(4)
O(1)–Ru(2)–N(6)	170.3(4)	O(3)–Ru(2)–N(4)	91.1(4)
N(4)–Ru(2)–N(5)	82.2(4)	O(3)–Ru(2)–N(5)	170.9(3)
N(4)–Ru(2)–N(6)	80.0(4)	O(3)–Ru(2)–N(6)	90.5(3)
N(5)–Ru(2)–N(6)	82.4(3)	O(3)–C(0)–O(4)	122.8(9)
O(4)–C(0)–O(5)	117.9(10)	O(3)–C(0)–O(5)	119.3(8)
Ru(2)–O(3)–C(0)	123.2(5)	Ru(1)–O(4)–C(0)	122.1(7)
Ru(1)–O(1)–Ru(2)	77.9(3)	Ru(1)–O(2)–Ru(2)	78.6(3)
O(1)–Ru(1)–O(2)	101.4(3)	O(2)–Ru(1)–O(4)	93.8(3)
O(1)–Ru(1)–O(4)	90.7(3)	O(2)–Ru(1)–N(1)	89.5(4)
O(1)–Ru(1)–N(1)	168.6(3)	O(2)–Ru(1)–N(2)	169.2(3)
O(1)–Ru(1)–N(2)	88.7(4)	O(2)–Ru(1)–N(3)	93.6(3)
O(1)–Ru(1)–N(3)	94.4(4)	O(4)–Ru(1)–N(1)	92.0(3)
N(1)–Ru(1)–N(2)	80.3(4)	O(4)–Ru(1)–N(2)	90.0(3)
N(1)–Ru(1)–N(3)	81.4(4)	O(4)–Ru(1)–N(3)	170.1(3)
N(2)–Ru(1)–N(3)	81.6(3)		

Complex **6**

Ru(1)–Ru(2)	2.469(1)	Ru(1)–O(1)	1.958(6)
Ru(1)–O(2)	1.952(6)	Ru(1)–N(1)	2.126(8)
Ru(1)–N(2)	2.105(8)	Ru(1)–N(3)	2.104(7)
Ru(1)–O(3)	2.061(7)	Ru(2)–O(1)	1.959(6)
Ru(2)–O(2)	1.955(6)	Ru(2)–N(4)	2.102(8)
Ru(2)–N(5)	2.115(8)	Ru(2)–N(6)	2.127(8)
Ru(2)–O(4)	2.043(7)	C(13)–O(4)	1.293(10)
C(13)–O(3)	1.317(11)	C(13)–O(5)	1.255(12)
O(2)–Ru(1)–N(3)	89.5(3)	O(2)–Ru(1)–N(1)	94.4(3)
N(2)–Ru(1)–N(3)	79.9(3)	O(1)–Ru(1)–N(2)	89.1(3)
O(1)–Ru(1)–O(3)	91.9(3)	N(1)–Ru(1)–N(2)	82.5(3)
N(1)–Ru(1)–O(3)	170.7(2)	O(1)–Ru(1)–N(3)	169.0(3)
N(3)–Ru(1)–O(3)	88.9(3)	N(1)–Ru(1)–N(3)	83.2(3)
O(2)–Ru(2)–N(4)	89.0(3)	O(2)–Ru(1)–O(3)	90.4(3)
O(1)–Ru(2)–N(5)	89.8(3)	N(2)–Ru(1)–O(3)	91.4(3)
N(4)–Ru(2)–N(5)	79.9(3)	O(1)–Ru(2)–O(2)	101.3(2)
O(1)–Ru(2)–N(6)	95.8(3)	O(1)–Ru(2)–N(4)	169.7(3)
N(4)–Ru(2)–N(6)	82.8(3)	O(2)–Ru(2)–N(5)	168.8(3)
O(2)–Ru(2)–O(4)	91.5(3)	O(2)–Ru(2)–N(6)	94.5(3)
N(5)–Ru(2)–O(4)	89.7(3)	N(5)–Ru(2)–N(6)	82.7(3)
Ru(1)–O(1)–Ru(2)	78.2(2)	O(1)–Ru(2)–O(4)	91.5(3)
N(6)–Ru(2)–O(4)	169.4(3)	N(4)–Ru(2)–O(4)	88.6(3)
Ru(1)–O(2)–Ru(2)	78.4(2)	Ru(1)–O(3)–C(13)	122.3(5)
O(3)–C(13)–O(5)	119.2(7)	O(5)–C(13)–O(4)	120.7(8)
O(3)–C(13)–O(4)	120.1(8)	C(13)–O(4)–Ru(2)	123.1(6)

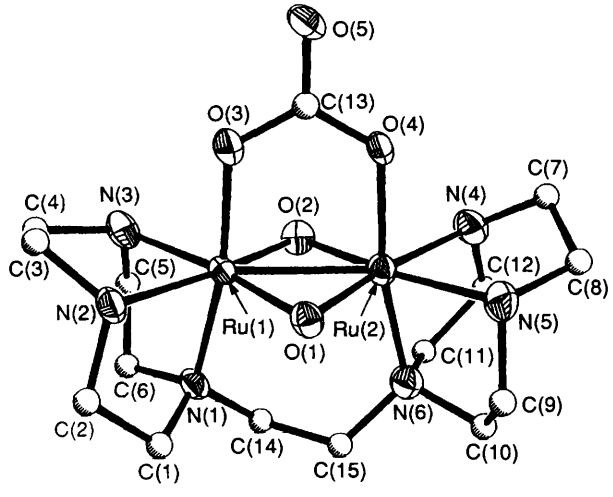

Fig. 5 Structure of the monocation in crystals of complex **6**

dications $[Ru_2(tacn)_2(\mu\text{-}OH)_2(\mu\text{-}CO_3)]^{2+}$, four bromide ions and seven molecules of water of crystallization per unit cell. The two ruthenium(III) ions are in a distorted-octahedral environment comprising a co-ordinated cyclic triamine, two hydroxo bridging groups and a μ-carbonato group. The overall geometry is very similar to that reported for the μ-acetato analogue $[Ru_2(tacn)_2(\mu\text{-}OH)_2(\mu\text{-}MeCO_2)]^{3+}$. The average Ru–N distance of 2.076 Å is within experimental error the same as for the μ-acetato complex (2.074 Å).[1] The same holds for the average $Ru–O_{hydroxo}$ distance which is 2.029, and 2.025 Å in the μ-acetato species. The Ru–Ru bond distance is rather short at 2.560(1) Å [2.572(3) Å in the μ-acetato complex] and in agreement with a bond order of one ($\sigma^2\pi^2\delta^2\delta^{*2}\pi^{*2}$). As has been pointed out previously,[10] the O–M–O and M–O–M bond angles of an edge-sharing bioctahedral transition-metal complex with two oxo or hydroxo bridges clearly respond to the presence or absence of metal–metal bonds: the former is acute and the latter is obtuse in cases with no metal–metal bonding; when such interactions are present, the former is often obtuse and the latter acute. This is clearly demonstrated by comparison of the metrical details of **5** with those reported for the isostructural complex $[Cr_2(tacn)_2(\mu\text{-}OH)_2(\mu\text{-}CO_3)]^{2+}$ where the Cr···Cr distance of 2.898 Å and Cr–O–Cr angles of 96.4° and O–Cr–O angles of 80.9° indicate the absence of a metal–metal bond.[11]

Although the protons of the bridging hydroxo groups have not been located in the structure of complex **5**, the $Ru–O_{hydroxo}$ distances at > 2.0 Å do not allow an assignment as oxo groups since the $Ru–O_{oxo}$ distance in all known crystal structures of μ-oxo-diruthenium(III) species is significantly shorter: *e.g.* in $[Ru_2(tmtacn)_2(\mu\text{-}O)(\mu\text{-}MeCO_2)_2]^{2+}$ this distance is 1.845 Å.[4a]

In the crystal structure of complex **5** there are a number of hydrogen-bonding contacts between the bromide ions and the amine protons of the co-ordinated triamine and between the water molecules of crystallization. These are listed in Table 6. Interestingly, the terminal oxygen atom of the bridging carbonate forms two weak hydrogen-bonding contacts to two water molecules [$O_w(1)$ and $O_w(2)$].

The overall geometry of the dinuclear monocation in crystals of complex **6** is quite similar to that described above for **5**. The amine dtne functions as a dinucleating ligand which binds two ruthenium ions connected by one μ-carbonato and two oxo bridges. The following structural differences between the first co-ordination spheres in both complexes allow an unambiguous assignment of bridging oxo in **6** rather than hydroxo groups in **5**: (*i*) the average $Ru–O_{oxo}$ bond distance at 1.956 Å is significantly shorter in **6** than the $Ru–O_{hydroxo}$ bonds in **5**; (*ii*) the average Ru–N distance in **6** is 0.037 Å *longer* than in **5** indicating thereby a structural *trans* influence of the oxo bridges on the Ru–N bonds in *trans* position. It is also noteworthy that the $Ru–O_{carbonato}$ bonds in both structures differ by 0.034 Å, those in **6** being *shorter* than those in **5**.

It is quite clear that removal of one electron and two protons from the $Ru^{III}_2(\mu\text{-}OH)_2^{4+}$ core in **5** forming thereby the mixed-valent cation **6** does not influence the corresponding bond

lengths in both cations other than by the differing π-donor capabilities of oxo *versus* hydroxo groups. It is therefore significant that the most pronounced effect of this chemical transformation occurs in the Ru–Ru bond distance which is *shorter* by 0.091 Å in **6** than in **5**. Note that the O–Ru–O angles of the oxo groups are obtuse and the Ru–O–Ru angles are acute in **5** and **6**.

We suggest that this shortening of the Ru–Ru distance is electronic in origin rather than steric as a consequence of the shorter $Ru–O_{oxo}$ bonds. The Ru–Ru bond order in complex **5** is one ($\sigma^2\pi^2\delta^2\delta^{*2}\pi^{*2}$); upon oxidation yielding **6** one electron is removed from an antibonding π* orbital giving rise to a bond order of 1.5 ($\sigma^2\pi^2\delta^2\delta^{*2}\pi^{*1}$). It is instructive to compare these results with those reported for a structurally characterized, similar pair of complexes[4a] namely $[Ru_2(tmtacn)_2(\mu\text{-}O)(\mu\text{-}MeCO_2)_2]^{2+}$ and $[Ru^{3.5}{}_2(tmtacn)_2(\mu\text{-}O)(\mu\text{-}MeCO_2)_2]^{3+}$ where the Ru · · · Ru distance *increases* from 3.258 to 3.342 Å ($\Delta = -0.084$ Å) upon one-electron oxidation despite the fact that the average $Ru–O_{oxo}$ distance *decreases* from 1.884 to 1.843 Å. This has been ascribed to very weak metal–metal bonding in both forms where the increased electronic repulsion between the two $Ru^{3.5}$ ions leads to a greater separation regardless of the increased Ru–Ru bond order. In contrast, the electronic repulsion between the two $Ru^{3.5}$ ions in **6** is effectively reduced by the two π-donating oxo bridges. In bioctahedral *face*-sharing $[Ru_2(tmtacn)_2(\mu\text{-}O)_3]^{2+}$ the Ru–Ru distance is very short at 2.401(2) Å indicating a metal–metal double bond ($\sigma^2\pi^4\pi^*{}_1\pi^*{}_2$) and in the edge-sharing bioctahedral complex $[L_{OEt}(HO)Ru^{IV}(\mu\text{-}O)_2Ru^{IV}(OH)L_{OEt}]$ $\{L_{OEt}{}^- = [(\eta^5\text{-}C_5H_5)Co\{(EtO)_2PO\}_3]^-\}$ this distance is 2.452(1) Å.[3] Thus it appears that in this class of edge-sharing complexes the Ru–Ru bond length decreases with increasing oxidation state on going from $Ru^{III}{}_2$ to $Ru^{3.5}{}_2$ to $Ru^{IV}{}_2$ complexes a Ru=Ru double bond may be envisaged ($\sigma^2\pi^2\delta^2\delta^{*2}$) rendering it diamagnetic.

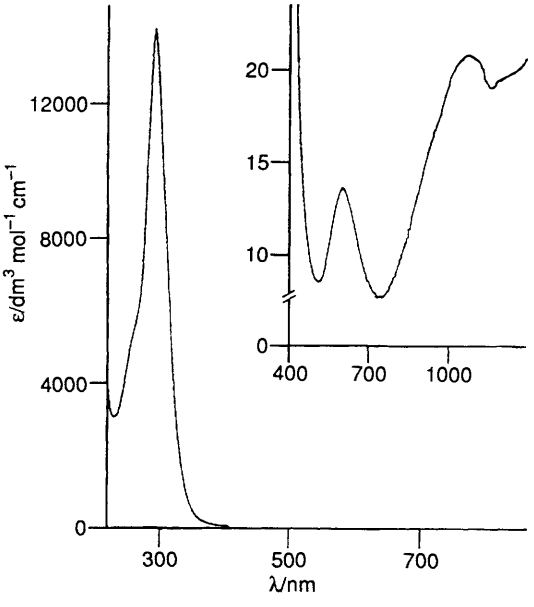

Fig. 6 Electronic spectrum of complex **5** in aqueous solution

Table 6 Hydrogen-bonding contacts (Å) in crystals of complexes **5** and **6**

Complex **5**			
O(1) · · · O_w(1)	2.602(9)	Br(1) · · · N(4)	3.307(7)
O(3) · · · O_w(3)	2.885(8)	Br(2) · · · N(5)	3.435(7)
O(5) · · · O_w(2)	3.013(9)	Br(1) · · · O_w(1)	3.200(7)
O(5) · · · O_w(1)	3.036(9)	Br(2) · · · N(3)	3.465(7)
O_w(1) · · · N(6)	3.267(9)	Br(2) · · · O_w(4)	3.215(7)
N(1) · · · O_w(2)	2.898(9)	Br(2) · · · O_w(3)	3.288(7)
O(4) · · · O_w(1)	2.710(9)	Br(1) · · · O_w(2)	3.262(7)
Complex **6**			
N(5) · · · O(7)	2.934(12)	N(4) · · · O(10)	2.962(12)
N(2) · · · O(6)	2.916(11)	N(3) · · · O(5)	2.833(13)

Electronic Spectra and Electrochemistry.—Electronic spectral and electrochemical data for the complexes are summarized in Tables 4 and 7, respectively. The cyclic voltammogram of $[Ru_2(dtne)(\mu\text{-}OH)_2(\mu\text{-}MeCO_2)][PF_6]_3$ has been recorded in aqueous solution at pH ≈7 (0.10 mol dm^{-3} $LiClO_4$, glassy carbon working electrode) in the potential range 0.00 to −0.80 V *vs.* normal hydrogen electrode (NHE). Two reversible one-electron transfer waves at $E^1{}_{\frac{1}{2}} = -0.35$ V and $E^2{}_{\frac{1}{2}} = -0.77$ V *vs.* NHE have been observed. Upon expansion of the potential range to −1.50 V a further irreversible one-electron reduction occurs at a more negative potential. This process has not been investigated further. In agreement with the cyclic voltammogram reported for $[Ru_2(tacn)_2(\mu\text{-}OH)_2(\mu\text{-}MeCO_2)]I_3\cdot H_2O$,[1] we assign the two reversible waves as in Scheme 2.

Interestingly, replacement of the two co-ordinated cyclic 1,4,7-triazacyclononanes in the latter complex by the dinucleating amine dtne renders the second reduction step to the $Ru^{II}{}_2$ dinuclear species reversible, indicating that dissociation of this species without a Ru–Ru bond to mononuclear species does not take place due to the ethane strap between the two 1,4,7-triazacyclononane moieties of dtne. On the other hand, this replacement does not affect the redox potential $E^1{}_{\frac{1}{2}}$ (and probably $E^2{}_{\frac{1}{2}}$); they are nearly the same for both species. The electronic spectra of these two $Ru^{III}{}_2$ dinuclear species are also very similar. This is evidence that the electronic configuration at the ruthenium ions is not significantly dependent on the presence or absence of the strap between the bound tacn ligands.

In contrast, the situation changes quite dramatically when the μ-carboxylato bridge is substituted by a μ-carbonato bridge. Fig. 6 shows the electronic spectrum of $[Ru_2(tacn)_2(\mu\text{-}OH)_2(\mu\text{-}CO_3)][PF_6]_2$ **5** in aqueous solution (pH 7) and Fig. 7 the

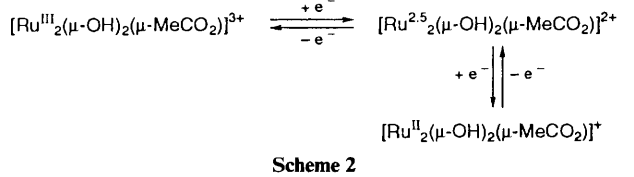

Scheme 2

Table 7 Electrochemical data for complexes

Complex	*E*/V *vs.* NHE	Ref.
$[Ru^{III}{}_2(tacn)_2(\mu\text{-}OH)_2(\mu\text{-}MeCO_2)][PF_6]_3$	−0.345 (r), −0.86 (i)	1
$[Ru^{III}{}_2(dtne)(\mu\text{-}OH)_2(\mu\text{-}MeCO_2)][PF_6]_3$	−0.35 (r), −0.77 (r)	This work
$[Ru^{III}{}_2(tacn)_2(\mu\text{-}OH)_2(\mu\text{-}CO_3)][PF_6]_2$	+0.90 (i), +0.83 (i), +0.54 (i), −0.46 (r)	This work
$[Ru^{3.5}{}_2(dtne)(\mu\text{-}O)_2(\mu\text{-}CO_3)]PF_6$	+0.56 (r), +0.12 (i), −0.20 (i), −0.58 (r)	This work

Cyclic voltammograms: glassy carbon working electrode; Ag–AgCl (saturated KCl–water) reference electrode; 0.10 mol dm^{-3} $LiClO_4$–water [complex] ≈ 10^{-4} mol dm^{-3}; scan rate 0.5–0.02 V s^{-1}; r = reversible; i = irreversible; scanned range, +0.4 to −1.3, +0.0 to −0.8, 1.0 to −1.0 V, and +0.9 to −0.8 V, *vs.* NHE for the four complexes respectively; the peak potentials of irreversible waves reported were recorded at a scan rate of 0.10 V s^{-1}.

cyclic voltammogram of **5** in aqueous 0.10 mol dm^{-3} $LiClO_4$ recorded at a glassy carbon working electrode. In the potential range 0.0 to −0.8 V one reversible one-electron reduction is observed as was judged from the diagnostic criteria [12] $\Delta(E_{pc} - E_{pa}) = 0.061$ V and $I_{p,red}/I_{p,ox} = 0.9$. When the potential range is expanded to 1.20 V *vs.* NHE an irreversible two-electron oxidation is observed at +90 V at a scan rate of 0.50 V s^{-1} and, concomitantly, two irreversible one-electron reduction peaks at +0.83 and +0.54 V (Fig. 7 bottom). Repeated scanning at the full potential range does not change the nature of the reversible one-electron-transfer wave. Thus the oxidation of **5** does not lead to mononuclear species but leads upon reduction by two electrons to the starting complex **5** which upon further one-electron reduction yields the mixed-valent form $[Ru^{2.5}{}_2(tacn)_2(\mu\text{-}OH)_2(\mu\text{-}CO_3)]^+$. Scheme 3 summarizes the proposed reactions.

Accordingly, the irreversible two-electron oxidation of complex **5** is accompanied by the loss of two protons from the hydroxo bridges yielding the μ-oxo-bridged complex $[Ru_2(tacn)_2(\mu\text{-}O)_2(\mu\text{-}CO_3)]^{2+}$. This oxidation was achieved coulometrically at +1.3 V *vs.* NHE and chemically by $[NH_4]_2[Ce(NO_3)_6]$. The resulting electronic spectra of these deep green solutions are identical and very similar to that shown in Fig. 3 which was generated by a reversible electrochemical one-electron oxidation of **6**. Thus we feel that complexes containing a $Ru^{IV}{}_2(\mu\text{-}O)_2(\mu\text{-}CO_3)^{2+}$ core are accessible. The full pH dependence of the above electrochemistry has not been investigated owing to decomposition of the μ-carbonato bridge at lower pH and, consequently, Scheme 2 is tentative. Interestingly, the redox potential for the reversible interconversion of $[Ru^{III}{}_2(\mu\text{-}OH)_2(\mu\text{-}MeCO_2)]^{3+/2+}$ occurs at a ≈100 mV more positive potential than for the corresponding species with a μ-carbonato bridge.

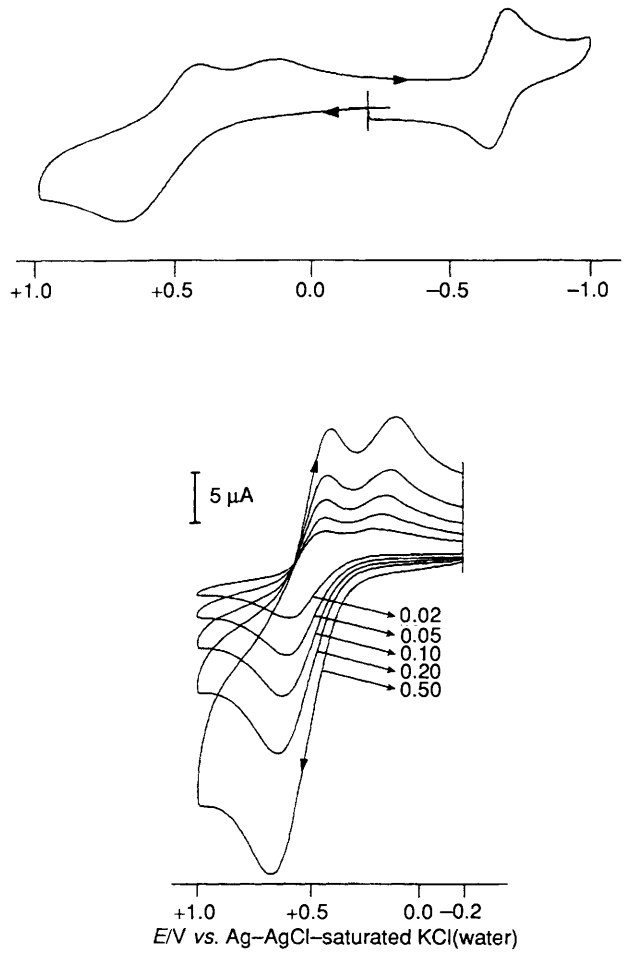

Fig. 7 Cyclic voltammograms of complex **5** in aqueous 0.10 mol dm^{-3} $LiClO_4$ solution. Top: in the range +1.2 to −0.8 V *vs.* NHE. Bottom: at different scan rates (0.02–0.50 V s^{-1}) in the range +1.2 to 0.0 V *vs.* NHE. Conditions: [complex **5**] ≈10^{-4} mol dm^{-3}; glassy carbon working electrode

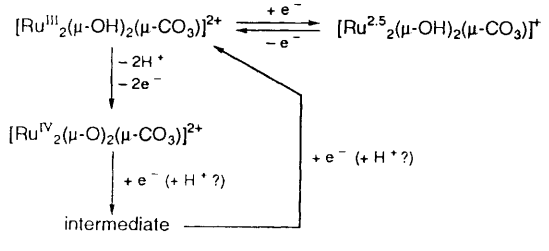

Scheme 3

Fig. 8 displays the cyclic voltammogram of complex **6** in an aqueous solution containing 0.10 mol dm^{-3} $LiClO_4$ as supporting electrolyte. In the potential range +0.90 to −0.80 V *vs.* NHE two reversible one-electron-transfer waves are observed at $E^1_{\frac{1}{2}} = +0.56$ V and $E^2_{\frac{1}{2}} = -0.58$ V *vs.* NHE which are coupled by an irreversible one electron reduction $E_{p,red} = -0.20$ V and oxidation $E_{p,ox} = +0.12$ V. Thus two reversible waves are coupled by two irreversible steps. The diagnostic criteria [12] for the reversible one-electron oxidation of **6** are clear: $\Delta(E_{p,ox} - E_{p,red}) = 0.057$ V and $I_{p,ox}/I_{p,red} = 1.02$. Coulometry at an oxidation potential of 0.70 V *vs.* NHE indicates the transfer of one electron ($n = 0.97$) and yields a deep green solution the electronic spectrum of which is shown in Fig. 3. The strong absorption maximum at 672 nm (ε = 840 $dm^3\ mol^{-1}\ cm^{-1}$) is characteristic for the $Ru^{IV}{}_2(\mu\text{-}O)_2(\mu\text{-}CO_3)^{2+}$ chromophore. One-electron reduction of such a solution at +0.40 V *vs.* NHE regenerates the mixed-valent μ-dioxo species **6**. The cyclic voltammogram of such a solution is identical to the one shown in Fig. 8. Further reduction of **6** by one electron is accompanied by an uptake of probably two protons generating $[Ru_2(dtne)(\mu\text{-}OH)_2(\mu\text{-}CO_3)]^{2+}$ which is not isolable but is completely analogous to **5**. It is therefore not surprising that the putative $Ru^{III}{}_2$ intermediate is reversibly reduced to $[Ru^{2.5}{}_2(dtne)(\mu\text{-}OH)_2(\mu\text{-}CO_3)]^+$ as is **5**. Both reversible processes occur at a very similar redox potential (Table 7). The proposed electrochemical reaction is summarized in Scheme 4. The pH dependence has not been studied because in the most interesting acidic regime decomposition of the μ-carbonato bridge is observed as is judged from the observed spectral changes of **5** and **6** in aqueous solutions pH <6. Although Schemes 3 and 4 must remain tentative we feel that together with the spectroscopic and other chemical data they do represent the observed behaviour correctly.

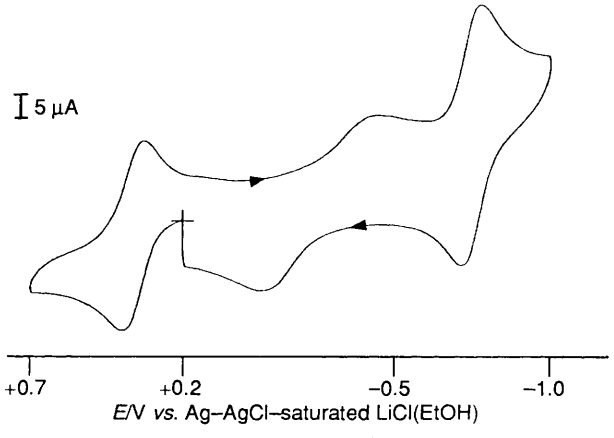

Fig. 8 Cyclic voltammogram of complex **6** (10^{-4} mol dm^{-3}) in aqueous solution (0.10 mol dm^{-3} $LiClO_4$) at a glassy carbon working electrode at a scan rate of 0.01 V s^{-1}

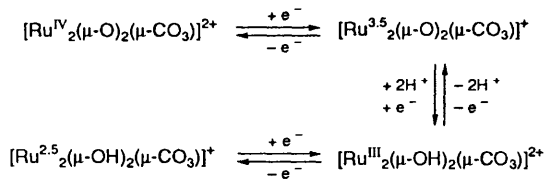

Scheme 4

Acknowledgements

We thank Drs. E. Bill and C. Butzlaff (Medizinische Universität Lübeck) for recording the ESR spectrum and the magnetic susceptibility and Dr. B. S. P. C. Della Vedova for performing many electrochemical experiments. This work was financially supported by the Fonds der Chemischen Industrie. We are grateful to Degussa (Hanau) for a generous loan of $RuCl_3 \cdot H_2O$.

References

1 K. Wieghardt, W. Herrmann, M. Köppen, I. Jibril and G. Huttner, *Z. Naturforsch., Teil B*, 1984, **39**, 1335.
2 P. Neubold, B. S. P. C. Della Vedova, K. Wieghardt, B. Nuber and J. Weiss, (*a*) *Angew. Chem., Int. Ed. Engl.*, 1989, **28**, 763; (*b*) *Inorg. Chem.*, 1990, **29**, 3355.
3 J. M. Power, K. Evertz, L. Henling, R. Marsh, W. P. Schaefer, J. A. Labinger and J. E. Bercaw, *Inorg. Chem.*, 1990, **29**, 5058.
4 (*a*) P. Neubold, K. Wieghardt, B. Nuber and J. Weiss, *Inorg. Chem.*, 1989, **28**, 459; (*b*) Y. Sasaki, M. Suzuki, A. Tokiwa, M. Ebihara, T. Yamaguchi, C. Kabuto and T. Ito, *J. Am. Chem. Soc.*, 1988, **110**, 6251; (*c*) B. K. Das and A. R. Chakravarty, *Inorg. Chem.*, 1990, **29**, 2078; (*d*) B. K. Das and A. R. Chakravarty, *Inorg. Chem.*, 1991, **30**, 4978; (*e*) A. Llobet, M. E. Curry, H. T. Evans and T. J. Meyer, *Inorg. Chem.*, 1989, **28**, 3131.
5 K. Wieghardt, I. Tolksdorf and W. Herrmann, *Inorg. Chem.*, 1985, **24**, 1230.
6 J. W. Richman and T. J. Atkins, *J. Am. Chem. Soc.*, 1974, **96**, 2268; K. Wieghardt, W. Schmidt, B. Nuber and J. Weiss, *Chem. Ber.*, 1979, **112**, 2220.
7 I. P. Evans, A. Spencer and G. Wilkinson, *J. Chem. Soc., Dalton Trans.*, 1973, 204.
8 G. M. Sheldrick, SHELXTL-PLUS, Universität Göttingen, 1990.
9 *International Tables for X-Ray Crystallography*, Kynoch Press, Birmingham, 1974, vol. 4, pp. 99, 149.
10 F. A. Cotton and R. A. Walton, *Multiple Bonds between Metal Atoms*, Wiley, New York, 1992.
11 K. Wieghardt, W. Schmidt, R. van Eldik, B. Nuber and J. Weiss, *Inorg. Chem.*, 1980, **19**, 2922.
12 R. S. Nicholson and I. Shain, *Anal. Chem.*, 1964, **36**, 706.

Received 28*th September* 1993; *Paper* 3/05833F